Phase instability induced by polar nanoregions in a relaxor ferroelectric system

GUANGYONG XU[1]*, JINSHENG WEN[1,2], C. STOCK[3] AND P. M. GEHRING[4]

[1]Condensed Matter Physics and Materials Science Department, Brookhaven National Laboratory, Upton, New York 11973, USA
[2]Department of Materials Science, State University of New York, Stony Brook, New York 11794, USA
[3]Department of Physics and Astronomy, The Johns Hopkins University, Baltimore, Maryland 21218, USA
[4]NIST Center for Neutron Research, National Institute of Standards and Technology, Gaithersburg, Maryland 20899-6100, USA
*e-mail: gxu@bnl.gov

Published online: 11 May 2008; doi:10.1038/nmat2196

Relaxor ferroelectrics are a special class of material that exhibit an enormous electromechanical response and are easily polarized with an external field. These properties make them attractive for applications as sensors and actuators. Local clusters of randomly oriented polarization, known as polar nanoregions (PNRs), are specific to relaxor ferroelectrics and play a key role in governing their dielectric properties. Here, we show through neutron inelastic scattering experiments that the PNRs can also significantly affect the structural properties of the relaxor ferroelectric $Pb(Zn_{1/3}Nb_{2/3})O_3$-4.5%$PbTiO_3$ (PZN-4.5%PT). A strong interaction is found between the PNRs and the propagation of acoustic phonons. A comparison between acoustic phonons propagating along different directions reveals a large asymmetry in the lattice dynamics that is induced by the PNRs. We suggest that a phase instability induced by this PNR–phonon interaction may contribute to the ultrahigh piezoelectric response of this and related relaxor ferroelectric materials. Our results naturally explain the emergence of the various observed monoclinic phases in these systems.

Understanding the effects of local inhomogeneities on the properties of materials has always presented a great challenge to condensed-matter physicists and materials scientists. The effort to elucidate the role played by local, polar clusters known as polar nanoregions (PNRs) that are observed in relaxor ferroelectrics is a prime example of such a challenge. Relaxor ferroelectrics (henceforth 'relaxors') belong to a special class of disordered materials that, because of their extraordinary piezoelectric and dielectric properties[1–3], show enormous potential for industrial applications such as next-generation sensors, actuators and transducers that convert between mechanical and electrical forms of energy. The inhomogeneities in these materials arise from chemical and valence mixing, and the resulting local polar structures can significantly affect macroscopic properties. For example, one of the defining features of relaxors—the broad and highly frequency-dependent dielectric permittivity peak—is directly associated with the relaxation process of the PNRs (ref. 4), which appear a few hundred degrees above the Curie temperature T_C (ref. 5). With cooling, the PNRs are believed to become larger in volume and/or more ordered in polarity. There have been extensive studies of the interplay between the PNRs and long-range polar order in relaxor systems[6–8]. On the other hand, the relationship between the PNRs and the electromechanical and other structural properties of relaxor systems remains unclear.

The structures of the PNRs have been well characterized in many lead-based, perovskite relaxor systems[9–14] and in particular in the prototypical relaxors $Pb(Zn_{1/3}Nb_{2/3})O_3$ (PZN) and $Pb(Mg_{1/3}Nb_{2/3})O_3$ (PMN) and their solid solutions with the conventional ferroelectric $PbTiO_3$ (PT). The local structure of PNRs is usually different from the average lattice structure of the compound in which they reside. For example, whereas the PNRs in PMN-xPT and PZN-xPT (for small x) exhibit orthorhombic ⟨110⟩ polarizations[14], the average macroscopic structure of these compounds is actually rhombohedral. Here, we establish a link between these different structures by studying the influence of the PNRs on the lattice dynamics in a relaxor system. In general, atoms in solids can move about their equilibrium positions and, through their motion, propagate energy in the form of sound waves or acoustic phonons. We find that the dynamics of relaxors is significantly influenced by these local inhomogeneities. Specifically, we have discovered a strong coupling between the PNRs and transverse acoustic (TA) phonons polarized along ⟨110⟩. The PNRs can scatter TA phonons having a parallel polarization; such phonons thus propagate more slowly and have shorter lifetimes. In other words, although the lattice of the bulk still remains virtually cubic (having only a slight rhombohedral distortion), the material itself can appear 'softer' along a particular ⟨110⟩ direction owing to the effects of the PNRs. Our work therefore provides a scenario wherein the interaction of the PNRs and the bulk lattice introduces an underlying structural instability, which could provide the microscopic origin of the large piezoelectric properties of relaxor systems.

The system we have studied is $Pb(Zn_{1/3}Nb_{2/3})O_3$-4.5%$PbTiO_3$ (PZN-4.5%PT), which lies on the left (rhombohedral) side of the morphotropic phase boundary (MPB) in the region of the PZN-xPT phase diagram where the ultrahigh piezoelectric response is observed; indeed, the piezoelectric coefficient d_{33} of this crystal is one of the highest known. Whereas a monoclinic phase can be induced in PZN-4.5%PT by applying an electric field along the [001] direction[15], under zero field it still exhibits a cubic high-temperature phase and a rhombohedral low-temperature phase, with a Curie temperature $T_C \sim 475$ K. Neutron inelastic scattering

© 2008 Macmillan Publishers Limited. All rights reserved.

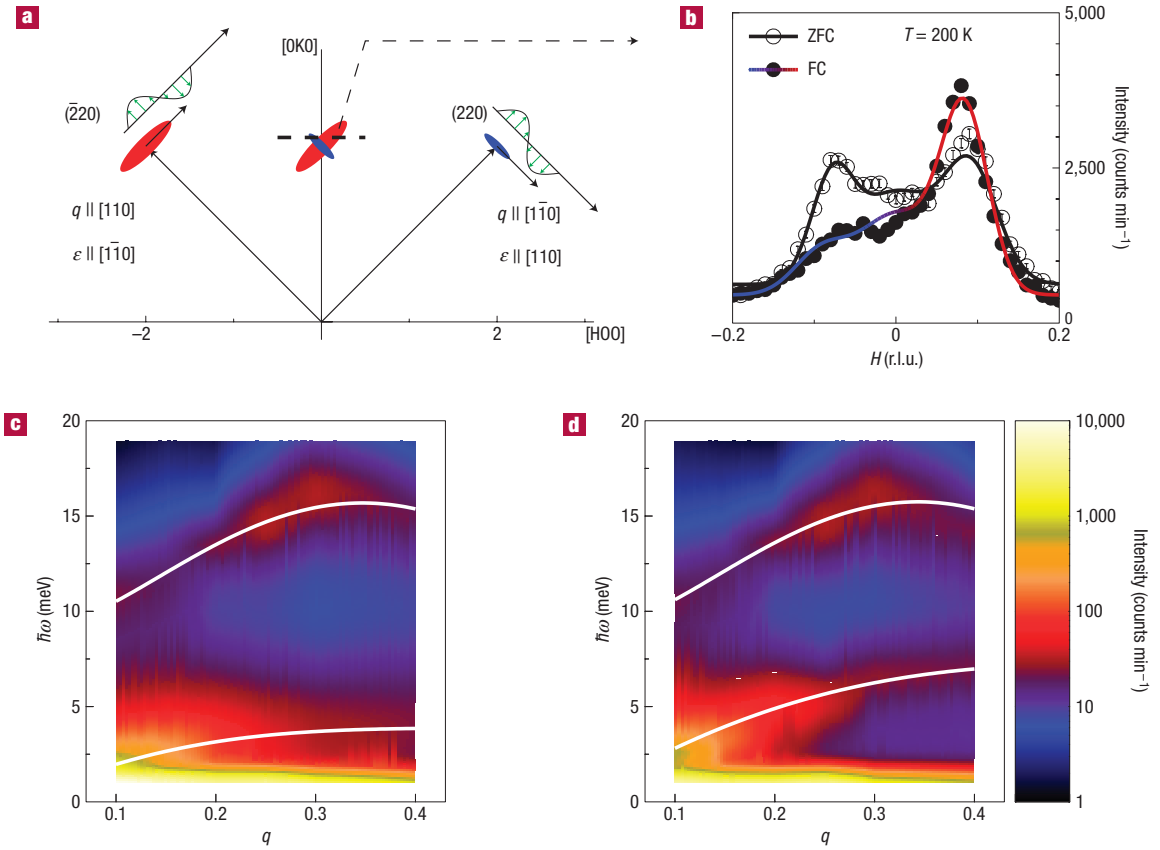


Figure 1 Neutron scattering measurements carried out on a PZN-4.5%PT single crystal with dimensions of 10 × 10 × 3 mm³. The experiment was carried out on the NCNR BT7 triple-axis spectrometer using beam collimations of 50′–50′–40′–240′. The final neutron energy was fixed at 14.7 meV. A pyrolytic graphite filter was placed after the sample to reduce higher-order neutrons. Lines are guides to the eye. **a**, A schematic diagram of the neutron scattering measurements, carried out near the (220) and ($\bar{2}$20) Bragg peaks. The blue and red ellipsoids represent the field-cooled (FC) diffuse scattering intensity distributions for *E* along [111]. The polarization and propagation vectors for the phonons are also noted. **b**, Profile of the diffuse scattering intensity measured along (*H* 2.1 0) (dashed line in **a**) under zero-field-cooled (ZFC) and field-cooled conditions. The error bars are obtained by taking the square root of the actual counts. **c**,**d**, Intensity contours measured near ($\bar{2}$20) (**c**) and near (220) (**d**).

measurements were carried out near the (220) and ($\bar{2}$20) Bragg peaks (expressed using pseudocubic notation) using the constant-**Q** method, that is, by scanning the neutron energy transfer $\hbar\omega$ while sitting at a fixed wave vector transfer **Q** located a distance **q** in reciprocal space from a given Bragg peak $\mathbf{G}(\mathbf{Q} = \mathbf{G} + \mathbf{q})$. It is important to note that both the PNR and phonon neutron scattering cross-sections involve the atomic displacements, whether static or dynamic; therefore, both cross-sections are subject to the factor $|\mathbf{Q}\cdot\boldsymbol{\varepsilon}|^2$, where $\boldsymbol{\varepsilon}$ is the unit vector along the polarization (atomic displacement) direction. Consequently, near the (220) (($\bar{2}$20)) Bragg peak, neutron scattering probes only those PNRs with [110] ([$\bar{1}$10]) polarizations as well as [110] ([$\bar{1}$10]) polarized phonons propagating along **q**. This situation is shown schematically in Fig. 1a, where **q** is chosen transverse to the Bragg peak **G** such that we measure TA phonons propagating along [110] and [1$\bar{1}$0] near ($\bar{2}$20) and (220), respectively.

When PZN-4.5%PT is zero-field-cooled, the diffuse scattering from PNRs forms ellipsoids[13,14] of equivalent shape and intensity centred on the (220) and ($\bar{2}$20) Bragg peaks. To identify the interaction between the PNRs and phonons explicitly, an ability to tune the diffuse scattering intensities independently and watch for changes in the phonon spectra is required. Fortunately, this can be achieved by cooling the single-crystal sample under a moderate external electric field $E = 2\,\mathrm{kV\,cm^{-1}}$ applied along [111]. When this is done, PNRs with different polarizations are reoriented, which leads to a redistribution of the diffuse scattering in reciprocal space[16] as shown in Fig. 1b. A linear scan of the scattering intensity measured along $[H, 2.1, 0]$ after field-cooling to 200 K (Fig. 1b) includes contributions from PNRs having both [110] and [$\bar{1}$10] polarizations and illustrates this redistribution. In other words, diffuse scattering intensities from PNRs having [110] polarizations (shown in blue in Fig. 1a,b) weaken, whereas those from PNRs having [$\bar{1}$10] polarizations (shown in red in Fig. 1a,b) strengthen when the system is field-cooled under a field applied along [111]. Remarkably, we find that the TA phonons polarized along [110] and [$\bar{1}$10] are significantly modified at the same time. Figure 1c,d shows contour maps of the phonon intensities measured near the (220) and ($\bar{2}$20) Bragg peaks after field-cooling to $T = 200$ K. Near (220), the lower-energy acoustic mode (the TA2 mode polarized along [110]) is sharp and well defined in energy, whereas the identical TA2 mode (but polarized along [$\bar{1}$10]) near ($\bar{2}$20) is comparatively very soft and broad. In contrast, the transverse optic (TO2) modes are essentially unaffected by the diffuse scattering as they do not differ noticeably between the two Bragg peaks.

Constant-**Q** scans are shown in Fig. 2 to provide a comparison between field-cooled and zero-field-cooled results at different temperatures. After cooling below T_C, a difference becomes noticeable between the zero-field-cooled (black solid lines) and

© 2008 Macmillan Publishers Limited. All rights reserved.

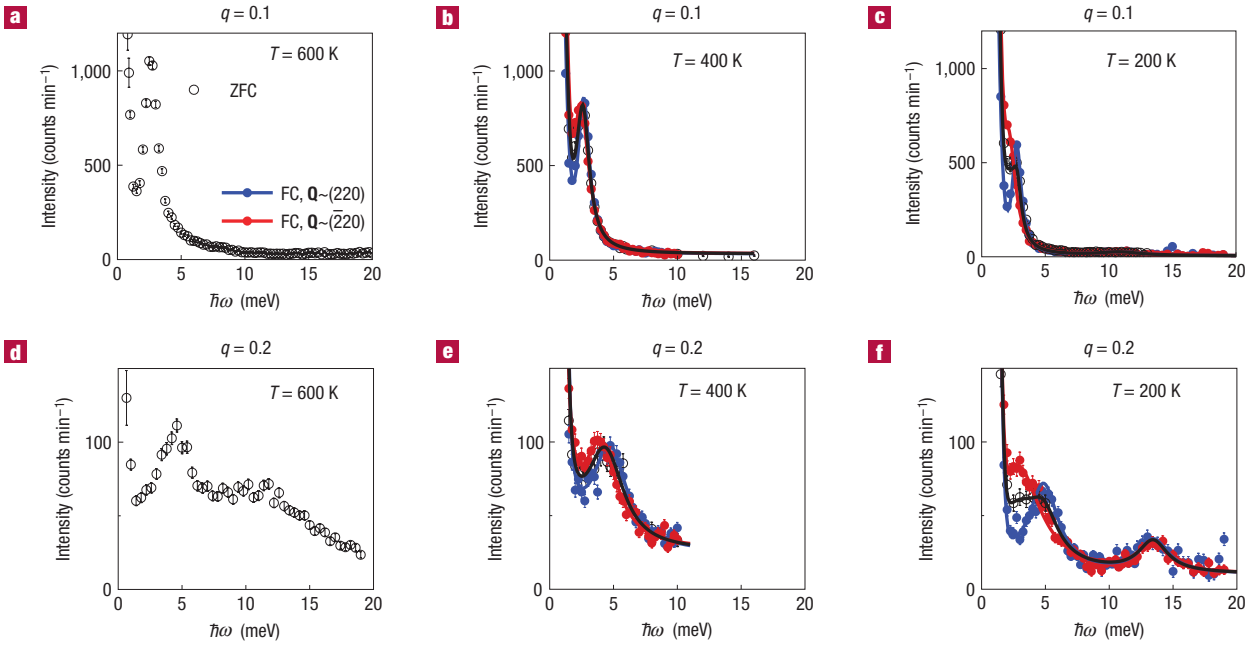


Figure 2 Constant-Q scans measured near the (220) and (2̄20) Bragg peaks at $q = 0.1$ and 0.2 r.l.u. The blue and red points are data taken near (2̄20) and (220) after cooling in a field $E = 2$ kV cm^{-1} oriented along [111]. The black points are zero-field-cooled data. Red and blue lines are guides to the eye. The black lines are calculated as an average of the two field-cooled data sets (blue and red data points), and can be compared directly to the zero-field-cooled data. The error bars are obtained by taking the square root of the actual counts.

field-cooled spectra measured near (220) (blue lines) and (2̄20) (red lines). At 400 K, the data in Fig. 2b,e show that where the diffuse scattering is strong (near (2̄20)), the corresponding TA2 phonon is soft and broad in energy; conversely, where the diffuse scattering is weak (near (220)), the TA2 mode is hard and well defined. These results unambiguously demonstrate the presence of a strong coupling between the diffuse scattering (PNRs) and the TA2 phonons in PZN-4.5%PT, evidence of which has also been observed in the relaxor PMN (ref. 17). If the PNRs grow on cooling, then this effect should become more pronounced at lower temperatures; the data in Fig. 2c,f, measured at 200 K, clearly show this to be the case.

It is important to note that if we average the two field-cooled phonon spectra measured below T_C near (220) and (2̄20) (represented by the black lines in Fig. 2), the result agrees almost exactly with the zero-field-cooled spectra. As our zero-field-cooled measurements were all carried out by heating the sample well above T_C and then cooling in zero field, any residue electric field effect or field-induced piezoelectric strain should have been completely removed. This shows that cooling under this moderate field merely rearranges the multiple ⟨111⟩-polarized ferroelectric domains such that the system adopts a single-domain state with polarization along the [111] field direction; any other effect of the field on the phonons or PNRs is negligible. In other words, the electric field does not soften or broaden the TA phonon modes, and the PNR–phonon coupling effect is intrinsic. If this were not true, then the average of the field-cooled spectra would not match the zero-field-cooled spectra. In the zero-field-cooled state, the effects of the PNRs on the phonon modes are still present (for $T < T_C$); however, because the zero-field-cooled data represent an average over different domains, the measurements made near (220) and (2̄20) cannot be distinguished.

The half-widths at half-maximum in energy of the TA2 phonons measured at 200 K are shown in Fig. 3c. The broad widths of the [1̄10]-polarized TA2 phonons indicate a short-lived mode. Although cooling in a field oriented along [111] stabilizes a single-domain rhombohedral phase, many PNRs having [1̄10] polarizations are present[16]; these PNRs seem to interact strongly with [1̄10]-polarized TA2 phonons, thereby reducing the phonon lifetime. However, because there are far fewer PNRs having [110] polarizations, the [110]-polarized TA2 phonons are relatively unaffected (Fig. 3a,c).

The data in Fig. 3a show that the TO2 mode is overdamped at small **q** at 600 K, in agreement with previous measurements on similar systems[18–20]; this q-dependent damping produces the dynamical feature known as the 'waterfall'. On cooling to 200 K, the optic modes harden and sharpen in energy (Fig. 3a,b), and are unaffected by the diffuse scattering changes below T_C, as can be seen by comparing the TO2 modes near the two Bragg peaks. This behaviour differs from the strong TA–TO coupling effects previously observed in similar systems at temperatures above T_C (refs 20,21). For $T < T_C$, the lack of any significant change in the TO modes compared with the large change in TA mode energies (between the two Bragg peaks) proves that any coupling between the TA and TO modes with ⟨110⟩ polarizations is extremely weak.

Phonons describe collective modes of atomic motions; acoustic phonons are directly associated with strains in the crystal lattice. A very soft and overdamped acoustic phonon mode is usually indicative of a phase instability and a tendency towards a structural transition. After the phase transition takes place and the system becomes stable, the phonon mode recovers and becomes well defined again. For instance, the softening of acoustic modes is common in other ferroelectric systems where the TA–TO coupling is strong, and the soft TA mode recovers after the structural phase transition takes place[22]. However, in PZN-4.5%PT, the structure remains rhombohedral for $T < T_C$. Although no phase transition associated with this [1̄10]-TA2 phonon anomaly ever occurs, the phonon mode remains anomalously soft and broad, and the

© 2008 Macmillan Publishers Limited. All rights reserved.

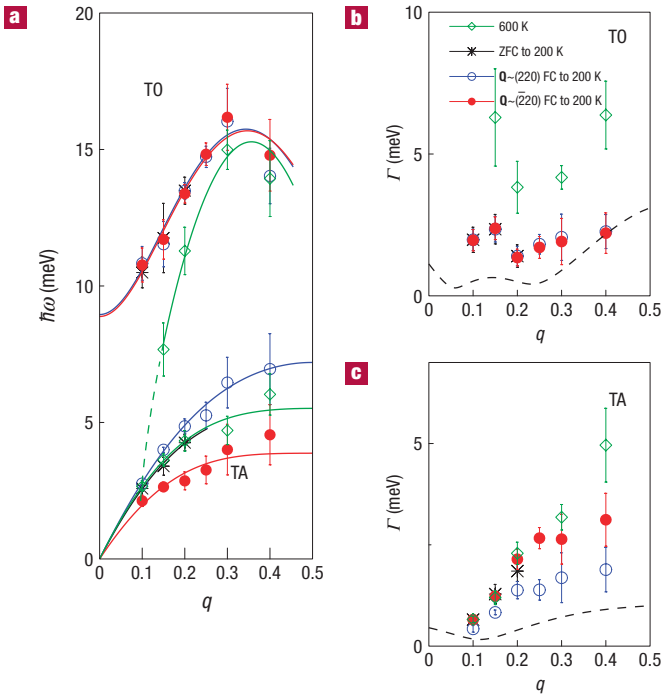


Figure 3 Phonon dispersions and energy widths (half-widths at half-maximum) measured around the (220) and (2̄20) Bragg peaks under field-cooled and zero-field-cooled conditions. The solid lines in **a** are guides to the eye. The dashed lines in **b**,**c** denote the instrumental energy resolution. The error bars are fitting errors obtained through least-squares fits to the data, assuming the phonon modes having lorentzian line shapes.

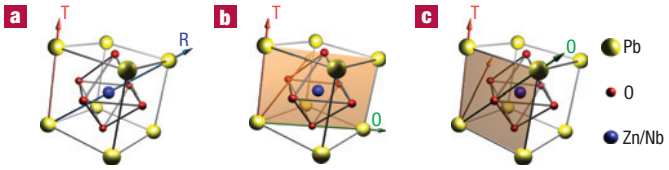


Figure 4 Schematic diagrams of the different polarization directions (marked by arrows) in the relaxor perovskite structure. a, Polarizations along the tetragonal (T) and rhombohedral (R) axes. **b**, The M_A phase, for which the polarization lies in the (110) plane, can be obtained by combining tetragonal and orthorhombic (O) strain. **c**, The M_C phase, for which the polarization lies in the (100) plane, can also be obtained by combining tetragonal and orthorhombic strain.

system remains (structurally) unstable at low temperature. In other words, the anomaly in this [1̄10]-TA2 mode is indicative of a phase instability in the low-temperature rhombohedral phase of PZN-4.5%PT.

Despite the large orthorhombic-type asymmetry between the TA2 phonon modes polarized along [110] and [1̄10], the static strain, or the deviation from a cubic structure, along these two orthorhombic directions in PZN-4.5%PT is small. The average structure of PZN-4.5%PT at low temperature is rhombohedral with a relatively small distortion with or without a moderate electric field applied along [111]. In our case, the static strain $\Delta d/d \leq 0.2\%$ along the [110] direction (determined from the size of the splitting between Bragg peaks—see also ref. 23); this is clearly not consistent with the large (>70%) difference in phonon energies between the two TA2 modes polarized along [110] and [1̄10], especially when compared with values observed in other relaxor/ferroelectric systems having similar structures. For example, in PMN-60%PT (ref. 24) at 400 K in the tetragonal phase, there is a much larger strain $\Delta d/d \sim 1.7\%$ along ⟨001⟩, whereas the splitting of the TA1 mode is less than 30% (estimated from the zero-field-cooled TA1 phonon broadening). Another example is the classic ferroelectric $PbTiO_3$, for which the tetragonal strain is about 6% at 200 K, whereas the TA1 phonons along the *a* and *c* directions only differ by ~20% in energy[25]. Note that these two systems have relatively large static strains, are both ferroelectric and show no evidence of PNRs. Intriguingly, similar to what we observe in PZN-4.5%PT, phonon studies on another relaxor system where PNRs are present, $K_{0.965}Li_{0.035}TaO_3$ ($x = 0.035$) (ref. 26), report a large splitting ($\Delta\omega \sim 25\%$ at $T = 4.8$ K) of the TA1 phonon modes polarized along the *a* and *c* directions as well, whereas the static tetragonal strain in that system is small (~0.2%). These examples suggest that in ferroelectric perovskites, the situation where a small static strain is accompanied by a large asymmetry in the lattice dynamics is unique to relaxors where PNRs are present. Once the external field and small static lattice strain have been excluded as origins of the anomalous asymmetry between TA modes measured at (2̄20) and (220), an interaction between the TA modes and the PNRs becomes the only viable explanation.

For materials to be considered 'good' piezoelectrics, it is not enough to exhibit a large static strain (for example, $PbTiO_3$ is not considered a good piezoelectric despite its large tetragonal strain); instead, a material must have a large derivative of strain with respect to external electric field, that is, the lattice/strain must be able to change significantly under field. Various previous theoretical, computational and experimental studies[27–31] have suggested a link between the phase instability in these compounds and the enhanced piezoelectric responses. In fact, acoustic phonons are directly related to the elastic constants in solids, and a soft TA mode is consistent with a system that is easier to distort (along a certain direction). Our results provide strong evidence that in relaxors such a phase instability does exist and is indeed induced by the PNRs and manifested as an asymmetry in the lattice dynamics. Note that this instability is intrinsic and not dependent on the external field (along [111]); the [111] field only rearranges large ferroelectric domains for the effect to be observed macroscopically as discussed previously. In the case of an external field oriented along [011] or [001], where the field direction does not align with the natural rhombohedral ([111]) domain polarization, the intrinsic instability apparently helps to facilitate the field-induced structural change and contributes to the large piezoelectric response[32]. Nevertheless, how or if the PNRs react to the field is not yet entirely clear; only very limited studies exist so far, such as ref. 33, and further study is required.

Although we have explicitly shown the existence of a strong PNR–phonon interaction in PZN-4.5%PT, this effect is not limited to one composition. It has been shown by neutron and X-ray diffuse scattering measurements that PNRs are present in all compositions to the left of the MPB in both PMN-*x*PT and PZN-*x*PT solid solutions[14,34] as well as for compositions inside the MPB (see Supplementary Information, Fig. S1). There is also evidence for a PNR–phonon interaction in other PT compositions such as PMN-20%PT (ref. 35) and pure PMN (ref. 17), where an anomalous TA phonon broadening has been observed and attributed to diffuse phonon coupling. Although PT doping towards the MPB or an external electric field[31] does enhance the electromechanical and piezoelectric properties in both PMN-*x*PT and PZN-*x*PT, the relaxor character itself plays an important and fundamental role. In fact, even in the absence of any PT, both pure PZN and PMN already exhibit extraordinarily high

© 2008 Macmillan Publishers Limited. All rights reserved.

field-induced piezoelectric strains[36]. With increasing PT content, some relaxor properties, such as the frequency dispersion in dielectric permittivity, are gradually suppressed; yet, the elastic diffuse scattering from PNRs is still present near the MPB. In fact, diffuse scattering measurements from PMN-*x*PT single crystals[34] have suggested that the **Q**-integrated diffuse scattering intensity increases with increasing PT and reaches a maximum near the MPB—precisely where the piezoelectric response is optimal, which is probably more than just coincidence. When these relaxor ferroelectric solid solutions cross the MPB into the tetragonal side of the phase diagram with even larger PT content, PNRs are no longer present[24,34] and the piezoelectric property drops markedly[1] (to values below even those of pure PMN and PZN).

The orthorhombic asymmetry in the lattice dynamics induced by the PNRs also has clear implications on the emergence of various monoclinic phases in relaxor ferroelectric solid solutions. Monoclinic phases[37–40] have been found in PMN-*x*PT and PZN-*x*PT for compositions near the MPB and can be induced in lower PT compositions with an external field applied along [001] (refs 41,42). These are believed to appear as a result of the 'polarization rotation' scheme proposed by Fu and Cohen[27]. Here, the polarization of the system can be rotated by an external field in a monoclinic plane, instead of being confined to a certain crystallographic orientation as in the rhombohedral or tetragonal phases (see Fig. 4 for details). Whereas PT doping tends to drive the system towards a tetragonal phase owing to the large tetragonal strain of $PbTiO_3$ itself, the low-symmetry monoclinic phases are considered as a bridge between the rhombohedral and tetragonal phases. One dilemma remains however. Intuitively, the bridging phase for low-PT rhombohedral and high-PT tetragonal phases should be M_A, where the polarization lies in the (110) plane (Fig. 4b); in reality, however, in both PZN-*x*PT and PMN-*x*PT systems, the zero-field phase near the MPB is M_C, not M_A (in fact, it is orthorhombic in PZN-*x*PT, which is a special case of M_C), where the polarization can rotate in the (100) plane (Fig. 4c). An M_C phase is also often observed when an electric field is applied along [001]. Using our results on the orthorhombic-type strain induced by PNRs, manifested by an asymmetry in the lattice dynamics, this situation can now be understood in simple phenomenological terms. The combination of a rhombohedral distortion and a tetragonal strain, either from PT doping or an external [001] field, can only produce an M_A phase; however, both M_A and M_C phases are possible (Fig. 4b,c) by combining tetragonal distortion with an orthorhombic strain instead.

In summary, we have shown that PNRs significantly affect the lattice stability in relaxor systems through a fundamental interaction with TA phonons. Although the average, static structure of the bulk is not explicitly modified by the PNRs, the local structure of the PNRs can be mapped onto the low-energy lattice dynamics macroscopically. The resulting relaxor phase has a nearly cubic structure with a large asymmetry in the lattice dynamics that also helps to explain intuitively the emergence of various monoclinic phases in relaxor ferroelectric solid solutions. Our results therefore provide evidence that the ultrahigh piezoelectric properties of relaxor ferroelectrics may arise from a structural instability resulting from a competition between the static bulk structure and local inhomogeneities that is mediated by acoustic phonons.

Received 10 October 2007; accepted 16 April 2008; published 11 May 2008.

References

1. Park, S.-E. & Shrout, T. R. Ultrahigh strain and piezoelectric behavior in relaxor based ferroelectric single crystals. *J. Appl. Phys.* **82**, 1804–1811 (1997).
2. Uchino, K. *Piezoelectric Actuators and Ultrasonic Motors* (Kluwer, Dordrecht, 1996).
3. Service, R. F. Shape changing crystals get shiftier. *Science* **275**, 1878 (1997).
4. Cross, L. E. Relaxor ferroelectrics. *Ferroelectrics* **76**, 241–267 (1987).
5. Burns, G. & Dacol, F. H. Crystalline ferroelectrics with glassy polarization behavior. *Phys. Rev. B* **28**, 2527–2530 (1983).
6. Blinc, R. *et al.* Local polarization distribution and Edwards–Anderson order parameter of relaxor ferroelectrics. *Phys. Rev. Lett.* **83**, 424–427 (1999).
7. Bokov, A. A. & Ye, Z.-G. Universal relaxor polarization in $Pb(Mg_{1/3}Nb_{2/3})O_3$ and related materials. *Phys. Rev. B* **66**, 064103 (2002).
8. Xu, G., Gehring, P. M. & Shirane, G. Coexistence and competition of local- and long-range polar orders in a ferroelectric relaxor. *Phys. Rev. B* **74**, 104110 (2006).
9. You, H. & Zhang, Q. M. Diffuse x-ray scattering study of lead magnesium niobate single crystals. *Phys. Rev. Lett.* **79**, 3950–3953 (1997).
10. Takesue, N., Fujii, Y. & You, H. X-ray diffuse scattering study on ionic-pair displacement correlations in relaxor lead magnesium niobate. *Phys. Rev. B* **64**, 184112 (2001).
11. La-Orauttapong, D. *et al.* Neutron scattering study of the relaxor ferroelectric $(1\text{-}x)Pb(Zn_{1/3}Nb_{2/3})O_3\text{-}xPbTiO_3$. *Phys. Rev. B* **67**, 134110 (2003).
12. Hlinka, J. *et al.* Diffuse scattering in $Pb(Mg_{1/3}Nb_{2/3})O_3$ with $PbTiO_3$ by quasi-elastic neutron scattering. *J. Phys. Condens. Matter* **15**, 4249–4257 (2003).
13. Hiraka, H., Lee, S.-H., Gehring, P. M., Xu, G. & Shirane, G. Cold neutron study on the diffuse scattering and phonon excitations in the relaxor $Pb(Mg_{1/3}Nb_{2/3})O_3$. *Phys. Rev. B* **70**, 184105 (2004).
14. Xu, G., Zhong, Z., Hiraka, H. & Shirane, G. Three dimensional mapping of diffuse scattering in $Pb(Zn_{1/3}Nb_{2/3})O_3\text{-}xPbTiO_3$. *Phys. Rev. B* **70**, 174109 (2004).
15. Noheda, B., Cox, D. E., Shirane, G., Gao, J. & Ye, Z.-G. Electric field induced phase transitions in $Pb(Zn_{1/3}Nb_{2/3})_{1-x}Ti_xO3$. *Phys. Rev. B* **65**, 224101 (2002).
16. Xu, G., Zhong, Z., Bing, Y., Ye, Z.-G. & Shirane, G. Electric field induced redistribution of polar nano-regions in a relaxor ferroelectric. *Nature Mater.* **5**, 134–140 (2006).
17. Stock, C. *et al.* Strong influence of the diffuse component on the lattice dynamics in $Pb(Mg_{1/3}Nb_{2/3})O_3$. *J. Phys. Soc. Japan* **74**, 3002–3010 (2005).
18. Gehring, P. M., Park, S.-E. & Shirane, G. Soft phonon anomalies in the relaxor ferroelectric $Pb[(Zn_{1/3}Nb_{2/3})_{0.92}Ti_{0.08}]O_3$. *Phys. Rev. Lett.* **84**, 5216–5219 (2000).
19. Shirane, G., Xu, G. & Gehring, P. M. Dynamics and Structure of PMN and PZN. *Ferroelectrics* **321**, 7–19 (2005).
20. Wakimoto, S. *et al.* Mode coupling and polar nanoregions in the relaxor ferroelectric $Pb(Mg_{1/3}Nb_{2/3})O_3$. *Phys. Rev. B* **66**, 224102 (2002).
21. Hlinka, J. *et al.* Origin of the 'waterfall' effect in phonon dispersions of relaxor perovskites. *Phys. Rev. Lett.* **91**, 107602 (2003).
22. Gehring, P. M. *et al.* Anomalous dispersion and thermal expansion in lightly doped $KTa_{1-x}Nb_xO_3$. *Ferroelectrics* **150**, 47–58 (1993).
23. Xu, G., Hiraka, H., Ohwada, K. & Shirane, G. Dual structures in PZN-xPT ferroelectric relaxors. *Appl. Phys. Lett.* **84**, 3975–3977 (2004).
24. Stock, C. *et al.* Damped soft phonons and diffuse scattering in $40\%Pb(Mg_{1/3}Nb_{2/3})O_3\text{-}60\%PbTiO_3$. *Phys. Rev. B* **73**, 064107 (2006).
25. Tomeno, I., Ishii, Y., Tsunoda, Y. & Oka, K. Lattice dynamics of tetragonal $PbTiO_3$. *Phys. Rev. B* **73**, 064116 (2006).
26. Toulouse, J. & Hennion, B. Inelastic-neutron-scattering study of the cubic-to-tetragonal transition in $K_{0.965}Li_{0.035}TaO_3$. *Phys. Rev. B* **49**, 1503–1506 (1994).
27. Fu, H. & Cohen, R. E. Polarization rotation mechanism for ultrahigh electromechanical response in single-crystal piezoelectric. *Nature* **403**, 281–283 (2000).
28. Wu, Z. & Cohen, R. E. Pressure induced anomalous phase transitions and colossal enhancement of piezoelectricity in $PbTiO_3$. *Phys. Rev. Lett.* **95**, 037601 (2005).
29. Budimir, M., Damjanovic, D. & Setter, N. Piezoelectric response and free-energy instability in the perovskite crystals $BaTiO_3$, $PbTiO_3$, and $Pb(Zr, Ti)O_3$. *Phys. Rev. B* **73**, 174106 (2006).
30. Frantti, J., Fujioka, Y. & Nieminen, R. M. Pressure-induced phase transitions in $PbTiO_3$: A query for the polarization rotation theory. *J. Phys. Chem. B* **111**, 4287–4290 (2007).
31. Kutnjak, Z., Petzelt, J. & Blinc, R. The giant electromechanical response in ferroelectric relaxors as a critical phenomenon. *Nature* **441**, 956–959 (2006).
32. Viehland, D., Amin, A. & Li, J. F. Piezoelectric instability in ⟨011⟩-oriented $PbB'_{1/3}B''_{2/3}O_3$–$PbTiO_3$ crystals. *Appl. Phys. Lett.* **79**, 1006–1008 (2001).
33. Gehring, P. M., Ohwada, K. & Shirane, G. Electric field effects on the diffuse scattering from $Pb(Zn_{1/3}Nb_{2/3})O_3$ doped with $8\%PbTiO_3$. *Phys. Rev. B* **70**, 014110 (2004).
34. Matsuura, M. *et al.* Composition dependence of diffuse scattering in the relaxor ferroelectric compound $(1-x)Pb(Mg_{1/3}Nb_{2/3})O_3\text{-}xPbTiO_3$ $(0 < x < 0.40)$. *Phys. Rev. B* **74**, 144107 (2006).
35. Koo, T. Y. *et al.* Anomalous transverse acoustic phonon broadening in the relaxor ferroelectric $Pb(Mg_{1/3}Nb_{2/3})_{0.8}Ti_{0.2}O_3$. *Phys. Rev. B* **65**, 144113 (2002).
36. Pan, W. Y., Gu, W. Y., Taylor, D. J. & Cross, L. E. Large piezoelectric effect induced by direct-current bias in PMN-PT relaxor ferroelectric ceramics. *Jpn. J. Appl. Phys.* **1**, 653–661 (1989).
37. Noheda, B. *et al.* Polarization rotation via a monoclinic phase in the piezoelectric $92\%PbZn_{1/3}Nb_{2/3}O_3\text{-}8\%PbTiO_3$. *Phys. Rev. Lett.* **86**, 3896–3899 (2001).
38. Cox, D. E. *et al.* Universal phase diagram for high-piezoelectric perovskite systems. *Appl. Phys. Lett.* **79**, 400–402 (2001).
39. Noheda, B., Cox, D. E., Shirane, G., Gao, J. & Ye, Z.-G. Phase diagram of the ferroelectric relaxor $(1-x)PbMg_{1/3}Nb_{2/3}O_3\text{-}xPbTiO_3$. *Phys. Rev. B* **66**, 054104 (2002).
40. La-Orauttapong, D. *et al.* Phase diagram of the relaxor ferroelectric $(1-x)PbZn_{1/3}Nb_{2/3}O_3\text{–}xPbTiO_3$. *Phys. Rev. B* **65**, 144101 (2002).
41. Ohwada, K., Hirota, K., Rehrig, P., Fujii, Y. & Shirane, G. Neutron diffraction study of field-cooling effects on the relaxor ferroelectric $Pb[(Zn_{1/3}Nb_{2/3})_{0.92}Ti_{0.08}]O_3$. *Phys. Rev. B* **67**, 094111 (2003).
42. Bai, F.-M. *et al.* X-ray and neutron diffraction investigations of the structural phase transformation sequence under electric field in $0.7PbMg_{1/3}Nb_{2/3}\text{-}0.3PbTiO_3$ crystal. *J. Appl. Phys.* **96**, 1620–1627 (2004).

Supplementary Information accompanies this paper on www.nature.com/naturematerials.

Acknowledgements

We would like to thank S. M. Shapiro and J. M. Tranquada for stimulating discussions. The financial support of the US Department of Energy under contract No. DE-AC02-98CH10886 and the Natural Science and Engineering Research Council of Canada (NSERC) is also gratefully acknowledged.

Author information

Reprints and permission information is available online at http://npg.nature.com/reprintsandpermissions. Correspondence and requests for materials should be addressed to G.X.

© 2008 Macmillan Publishers Limited. All rights reserved.